Available online at www.sciencedirect.com
SCIENCE DIRECT®
C. R. Physique 4 (2003) 891–899
COMPTES RENDUS PHYSIQUE

The Cosmic Microwave Background/Le rayonnement fossile à 3K

Extragalactic contributions to the CMB signal

Guilaine Lagache, Nabila Aghanim

IAS, bâtiment 121, Université de Paris XI, 91405 Orsay cedex, France

Presented by Guy Laval

Abstract

One of the main challenges facing upcoming Cosmic Microwave Background (CMB) experiments aiming at measuring temperature anisotropies with great accuracy will be to assess the contamination of CMB measurements by galactic and extragalactic foregrounds. On the extragalactic side, confusion noise from extragalactic sources hampers the detection of intrinsic CMB anisotropies at small angular scales. Secondary CMB anisotropies must also be carefully accounted for in order to isolate the primordial fluctuations. We present in this article a brief overview of the extragalactic contributions to the CMB. The galactic foregrounds are discussed elsewhere (Giard and Lagache, this issue). ***To cite this article: G. Lagache, N. Aghanim, C. R. Physique 4 (2003).***

Résumé

Avant-plans extra-galactiques au CMB. La mesure des anisotropies du Fond Diffus Cosmologique Micro-onde a fait de considérables progrès ces 10 dernières années, grâce notamment aux remarquables avancées technologiques. Nous entrons aujourd'hui dans l'ère de la cosmologie de précision. Dans ce contexte, la contamination par les avant-plans galactiques et extra-galactiques devient un élément critique qu'il faut parfaitement maîtriser. Côté extragalactique, les galaxies lointaines (les radio-galaxies et les galaxies infrarouge) polluent la détection des anisotropies du FDCM aux petites échelles angulaires. Superposées aux anisotropies primaires du FDCM, les anisotropies dites secondaires, qui proviennent après la recombinaison de l'interaction des photons avec la matière des régions ionisées et/ou chaudes ou avec le potentiel gravitationnel des structures, doivent être proprement prises en compte afin d'isoler les anisotropies primaires. Ce papier présente un résumé de ces avant-plans extra-galactiques. La revue de la contamination des anisotropies du FDCM par les émissions provenant de notre Galaxie est également présentée dans ce volume (Giard et Lagache). ***Pour citer cet article : G. Lagache, N. Aghanim, C. R. Physique 4 (2003).***

Keywords: CMB primary anisotropies; Secondary anisotropies; Galaxies; Cosmology; Early Universe

Mots-clés : Anisotropies du fond diffus ; Anisotropies secondaires ; Galaxies ; Cosmologie ; Univers primordial

1. Introduction

Within the context of standard cosmological models, the formation and evolution of the cosmic structures observed today are based on two hypotheses. The first is the presence of density perturbations with respect to the average matter distribution: the so-called primordial density fluctuations. The second is that these initial perturbations grow through gravitational instability. Before recombination, at redshift $z \simeq 1100$, matter and radiation were tightly coupled. The Cosmic Microwave Background (CMB) represents an image of the photon distribution at the recombination and thus of the underlying density fluctuations.

E-mail addresses: guilaine.lagache@ias.u-psud.fr (G. Lagache), nabila.aghanim@ias.u-psud.fr (N. Aghanim).

1631-0705/$ – see front matter
doi:10.1016/j.crhy.2003.09.010

As a consequence, the CMB anisotropies (called primary in this case) are a powerful tool as they probe both the early Universe and the structure formation model. However and in addition to the instrumental effects, there are several astrophysical contributions that could disturb the primordial cosmological signal. In fact, after recombination, the CMB photons interact along their path with the matter in the ionised and/or hot regions (scattering effects, Section 2), or with the gravitational potentials of structures (gravitational effects, Section 3). These interactions produce the so-called secondary temperature fluctuations, which superimpose to the primary anisotropies. Secondary fluctuations must be carefully accounted for in order to isolate the primordial fluctuations. Moreover, they are interesting in their own since they provide additional constraints on the 'local' properties of the universe.

The other sources of contamination to the primary CMB anisotropies are the extragalactic point sources. We can distinguish two classes of point sources that hamper the detection of the CMB anisotropies at small scales (typically galactic scales): the so-called radio sources and the dusty galaxies (detailed in Section 4). Note, however, that the clustering of these sources can moreover produce extra power at larger scales as discussed in Section 5.

2. Secondary anisotropies due to scattering

2.1. The Sunyaev–Zel'dovich effect

The SZ effect (e.g., [1] for a review) was introduced by Sunyaev and Zel'dovich in 1972 to designate the inverse Compton interaction of the CMB photons with the free electrons of the hot gas pervading the clusters of galaxies. It is usually 'decomposed' into: the Thermal SZ (TSZ) which is the inverse Compton effect and the Kinetic SZ (KSZ) due to the Doppler effect of the moving cluster. The TSZ amplitude is a measure of the pressure integral along the line of sight (l.o.s.) directly linked to the intra-cluster gas properties (temperature T_e and optical depth τ). It has a peculiar spectral signature (Fig. 1) with an excess of brightness at high frequencies (>217 GHz) and a decrement at low frequencies (<217 GHz). In the non-relativistic approximation, this spectral signature is universal, whereas it varies with T_e in the exact computations including the relativistic corrections and multiple scattering (e.g., [3] and references therein). The KSZ effect corresponds to a first-order Doppler effect when a galaxy cluster moves with respect to the CMB rest frame with a radial peculiar velocity v_r. The KSZ fluctuations have the same spectral signature as the primary CMB anisotropies (Fig. 1) with amplitudes proportional to the product $v_r \times \tau$.

The SZ effect of galaxy clusters is one of the major sources of secondary anisotropies. It is also a potentially powerful tool for cosmology. Due to its spectral signature, the TSZ can be separated from the other components by means of accurate multi-wavelength observations in the mm and submm ranges (e.g., [4]). As proposed initially by [5], v_r can be inferred from SZ measurements. Nevertheless, the accuracy on individual clusters is limited by confusion with other components of the microwave sky (CMB principally). In this context, averaging over many clusters in large volumes might in turn measure the bulk motions and the large scale velocity fields [6]. In combination with X-ray and gravitational lensing observations, the TSZ effect enables us to study the gas distribution and cluster dynamical state, and in addition to constrain cosmological parameters such as the gas fraction and the Hubble constant (e.g., [7–9]). The SZ effect is distant independent that makes it a particularly powerful tool for detecting high redshift clusters. The SZ cluster counts can thus probe the cosmological model, e.g., the matter density of the universe and the dark energy content (e.g., [10,11]).

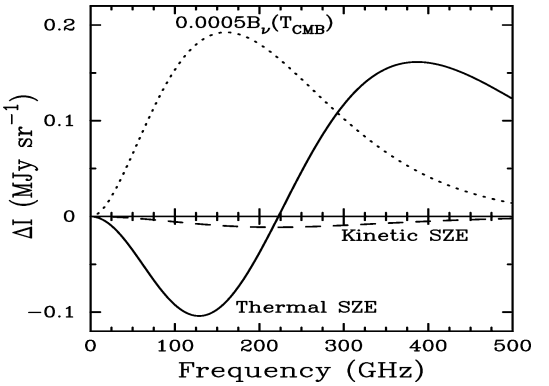

Fig. 1. Intensity of the spectral distortion of the CMB due to SZ effect ($T_e = 10$ keV, Compton y parameter is 10^{-4}, and $v_r = 500$ km·s^{-1}, from [2]). The thick solid line is the TSZ and the dashed line is the KSZ. Note that the KSZ fluctuations have the same spectral signature as the primary CMB anisotropies. The 2.7 K thermal spectrum for the CMB scaled by 0.0005 is shown by the dotted line.

In order to fulfill these objectives several experiments have been built using single dish radio telescopes, e.g., OVRO-40 m telescope, bolometric instruments, e.g., PRONAOS and DIABOLO or interferometric techniques, e.g., Ryle telescope and BIMA-OVRO projects (see [2] for details). The latter have now allowed us to obtain quasi-routinely high quality SZ data on clusters with $0.2 < z < 0.9$. Future experiments are already planned to perform SZ surveys and constrain the cosmological model: AMIBA, ACBAR, Planck, ACT,...). They might give us, in particular, a precise measure of the SZ contribution to the CMB power spectrum at small scales, provided the sensitivity, the frequency coverage and the angular resolution allow a good component separation. At present, only analytic or semi-analytic computations and numerical simulations are used to predict the SZ power spectrum (e.g., [12,13] and references therein). They show an important scatter which does not quite explain, within present cluster normalisation, the excess of power at small scales measured by CBI, BIMA and VSA.

The TSZ distortions originate from the hot gas in clusters. However more generally, it can be associated with any ionised hot medium along the l.o.s. As a matter of fact, the *COBE-FIRAS* experiment, which put an upper limit to the mean Compton parameter [14], found it one order of magnitude higher than the predicted contribution from the intra-cluster gas only. It thus leaves room for other contributions to the global Compton distortion (e.g., Section 4.4).

2.2. Inhomogeneous re-ionisation

Recent observations show that the Universe underwent a re-ionisation that was completed at redshift $z_i \sim 6$ and started probably earlier, $z \simeq 20$. The evidence for total re-ionisation relies on observations showing the absence of neutral hydrogen towards distant ($z_i \sim 6$) quasars in the SLOAN survey (e.g., [15,16]) as well as on the recent WMAP measurement [17]. The re-ionisation of the Universe is intimately related to the history of structure formation. In the commonly accepted picture, the re-ionisation is indeed achieved by the photo-ionisation of initially neutral gas by early luminous sources (stars, quasars, dwarf galaxies) which ionise hydrogen atoms in their vicinities. The re-ionisation thus starts as an inhomogeneous process, and the total re-ionisation is reached when the ionised bubbles overlap (due to their increasing number and to their expansion). As pointed out by [18], the inhomogeneous re-ionisation (IHR) can induce secondary anisotropies of the KSZ type, when the ionised bubbles move with respect to the CMB rest frame. The temperature inside the ionised bubbles is very low so that the amplitude of the induced TSZ anisotropies is quite negligible. Therefore, an important question from the point of view of CMB, is the effects of IHR in terms of induced temperature fluctuations. The contribution of the IHR to the total anisotropies in terms of power spectrum has been predicted analytically by [18] (Fig. 5) (see also the empirical model of [19]). It was also computed from numerical simulations (e.g., [20,21]). Its amplitude (a few to a few tens of μK) together with its scale range (a few to a few tens of arcminutes) are still rather scattered. Indeed, both depend on the redshift at which ionisation started and on the typical size of the ionised bubble (i.e., the type of ionising sources and their number counts). Small (large) bubbles, shift the power spectrum to smaller (larger) angular scales and decrease (increase) its amplitude.

2.3. The Ostriker–Vishniac effect

Alongside with the IHR fluctuations produced during the first stages of re-ionisation and independently of any model of ionisation, some secondary fluctuations arise from the so-called Ostriker–Vishniac effect (OV) [22,23] during the linear regime of the density fluctuations evolution. Contrary to the IHR, this second order effect is due entirely to a Doppler effect with a modulation of the velocity field by spatial variations of the density field. This in turn affects the probability of scattering. Estimates of the OV power spectrum, and its contribution to the temperature anisotropies were given by several authors (e.g., [24,25]). Due to its density squared weighting, the OV effect peaks at small angular scales, typically arcminute scales, and produces μK rms temperature anisotropies (Fig. 5). This effect will be very hard to distinguish from other Doppler induced secondary fluctuations.

3. Secondary anisotropies due to gravitational interaction

The climbing of CMB photons in and out time-varying gravitational potentials induces a differential redshift. Its effect along the l.o.s. is called the Integrated Sachs–Wolfe [49] effect (ISW). Its non-linear contribution is due to large scale structure evolution and is known as the Rees–Sciama [48] effect (RS) (see [26] and Fig. 5). In addition, the transverse motion of the dark matter halos across the l.o.s. leads to a dipolar temperature anisotropy of a few μK (e.g., [27,28]). The CMB photons are also affected by gravitational lensing. Gravitational lensing by large scale structures redistributes the power among scales. It smoothes the acoustic peaks at large angles and moves the power to small ones.

4. Extragalactic point sources in the (sub-)millimeter

The millimeter range corresponds to a minimum in the Spectral Energy Distribution (SED) of our Galaxy and of most classes of extragalactic sources. As illustrated in Fig. 2, the minimum is situated around 3 mm, the crossing-point of the decreasing dust emission ($I_\nu \propto \nu^\alpha$ with $\alpha = 3$ to 4) and the increasing radio emission ($I_\nu \propto \nu^\alpha$ with $\alpha = -0.5$ to -1, generally). Because of such steep variation with frequency, the position of the minimum does not depend much on the relative contribution of the two components. Due to their different physical nature, the predominance of one of the components, i.e., thermal radiation by dust or synchrotron emission, gives birth to dusty galaxies (Section 4.2) or radio-galaxies (Section 4.3), respectively.

4.1. Source counts

There is, in the millimeter domain, a lack of large surveys for both classes of objects, radio sources and dusty galaxies. Counts of radio sources are presently available only at cm wavelengths. Deep VLA surveys have allowed to extend direct determinations of radio source counts down to μJy at 1.41, 4.86 and 8.44 GHz. At these frequencies, the counts span about 7 orders of magnitude in flux. Although very well constrained in the cm, the extrapolation to the mm is subject to large uncertainties. The most critical point is the assumption on source spectra since a large variety of radio sources (such as radio-loud AGN, quasars, blazars) is expected to dominate the counts at mm wavelengths. For dusty galaxies, counts are presently available at 15, 170, 850 and 1300 μm. At 15 μm, thanks to *ISO* observations, counts span more than 2 orders of magnitude [30]. On the other hand, for $\lambda \geqslant 850$ μm, since surveys are limited to small areas and are confusion limited at about 2 mJy, the counts span only about 1 order of magnitude. Different coherent models now reproduce the counts from mid-IR to the millimeter wavelengths (e.g., [31]). The details of the modeling give, however, different results on important issues such as the redshift distribution of sources and their contributions to the fluctuations.

Our current best guess for counts in some (sub-)mm channels is given in Fig. 3. In the millimeter, counts at high fluxes are dominated by radio sources. As we move towards fainter fluxes, we probe dusty galaxies with extreme star formation activity up to 10^3 $M_\odot$/yr. With future all-sky survey missions, such as *Planck*, only bright sources will be detected. Unresolved fainter sources will contribute to the fluctuations at small scales (see Fig. 4).

4.2. Dusty galaxies

Dust absorbs UV and optical light from stars and reradiates from few μm to mm (for convenience, this wide wavelength domain will be called InfraRed (IR) in the following). First systematic observations of local IR galaxies has been done by the *IRAS* satellite, launched in 1983. *IRAS* showed that galaxies can be classified in a luminosity sequence from spirals to Luminous IR Galaxies (LIRGs, $10^{11} < L_{IR} < 10^{12} L_\odot$) and Ultra Luminous IR Galaxies (ULIRGs, $L_{IR} \geqslant 10^{12}$ $L_\odot$) that radiate more than 95% of their bolometric luminosity in the IR. Moreover, we know, from *IRAS* observations that about 30% of the bolometric luminosity of local galaxies is radiated in the IR [34]. In 1996, the controversial discovery of a very bright Cosmic IR Background (CIB, [35]), then confirmed by other studies (see [36–41]), showed that the situation changes dramatically as

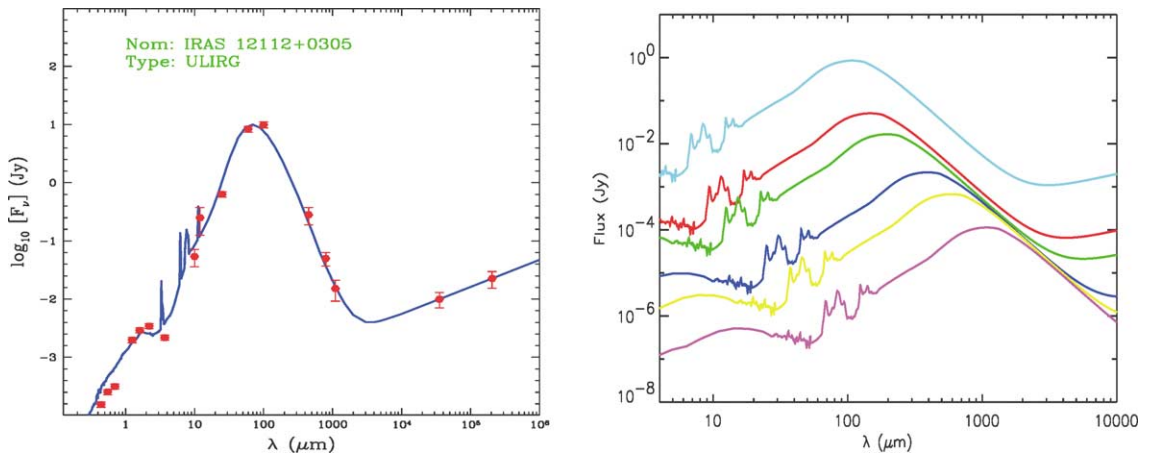

Fig. 2. Left: Spectral Energy Distribution of an ULIRG ($L_{IR} = 3.4 \times 10^{12}$ $L_\odot$). The solid line shows the fit of the data with a theoretical spectrum computed by [29]. Right: Observer-frame model spectrum of a $L_{IR} = 5 \times 10^{11}$ $L_\odot$ galaxy at increasing redshift (0.1, 0.5, 1, 3, 5 and 10): illustration of the so-called negative-K correction at mm wavelengths.

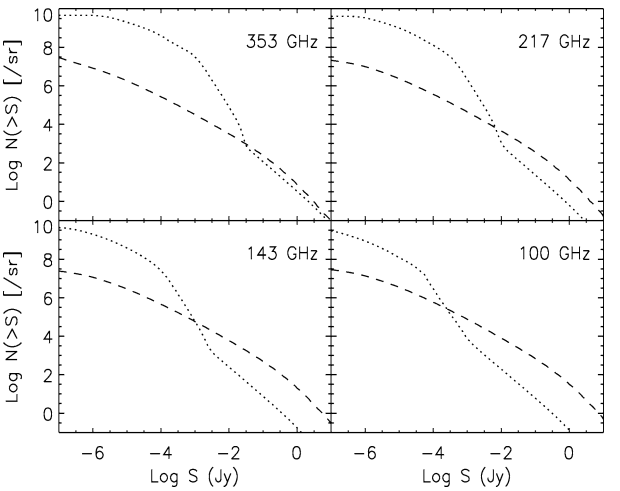

Fig. 3. Predicted counts at 353, 217, 143 and 100 GHz. The dashed and dotted line show the contributions of radio (from [32]) and far-IR (from [31]) selected sources.

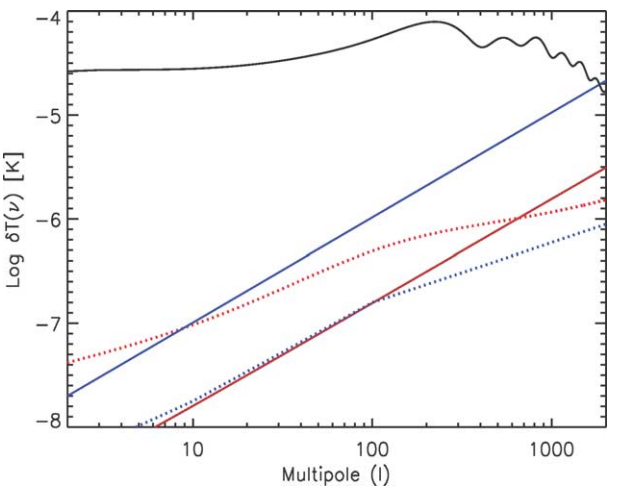

Fig. 4. Predicted angular power spectrum of the extragalactic point source contaminants at 100 GHz. For each component we plot $\delta T(\nu) = [l(2l+1)C_l(\nu)/4\pi]^{0.5}$. The black solid line are the CMB primary anisotropies. The blue and red solid lines are the Poissonnian fluctuations of the radio and dusty galaxies respectively (sources with fluxes greater than 1 Jy are assumed to be identified and removed). The blue and red dotted lines are estimates of the clustering of radio sources (extracted from [33]) and dusty galaxies (L. Knox, private communication), respectively.

we go to higher redshifts. The CIB originates from the accumulation of dust emission from more or less distant star-forming galaxies and/or Active Galactic Nucleis (AGN) along each l.o.s. The re-emitted dust radiation in the CIB contains at least as much total power as the optical/near-IR background (present measurements give a factor of about 2). This ratio is much larger than what was measured locally by *IRAS* (40%, see above). The CIB is thus likely to be dominated by redshifted IR galaxies. Probing the population that makes up the CIB is thus of crucial importance to understand when and how the bulk of stars formed in the Universe. Several deep cosmological surveys at 15, 170, 850 and 1300 μm have, to various extents, resolved the CIB into discrete sources. The two main results are: (1) most of the IR sources are powered by starbursts with high star formation rates (from few tenths to few hundreds) and (2) number counts indicate a very strong cosmological evolution of IR galaxies. This evolution is likely to be associated with the merging history of galaxies – IR galaxies making the bulk of the background show complex structures and morphological peculiarities, signs of past or present interaction or merging. Thus, resolved IR galaxies together with their unresolved contribution are likely to be associated with the densest parts of the Universe. These galaxies at long wavelength (i.e., $\lambda \geqslant 800$ μm) probe to higher redshift thanks to the so-called 'negative-K' correction, arising from the counterbalance of the distance effect by the emission maximum that peaks at ∼80 μm in the rest-frame (Fig. 2). The mm

domain is thus very sensitive to the early-stages of galaxy evolution. *Planck* will resolve only perhaps 5% of the CIB into sources, but additionally has the sensitivity for detecting its correlated fluctuations. Observing these fluctuations will allow a determination of physical properties of contributing galaxies and their bias relative to the dark matter density field. Analyses of these fluctuations have implications on the typical galaxy mass scales and on the formation of bulges or groups, for example.

Understanding the physical and evolutionary properties of the IR galaxies is still a major challenge. Detailed contribution of AGNs dust heating and starburst is still unsolved, as well as the contribution of gravitational lensing. Moreover, semi-analytic models, in the paradigm of hierarchical structure formation, and tuned to agree with detailed numerical simulations are unable to account for the sub-(mm) counts of galaxies. This can have large impacts on CMB studies. Any uncertainty in the modeling of galaxy evolution at high redshift will strongly affect the faint galaxy counts in the mm (due to the negative-K correction) and thus their contribution to the fluctuations.

4.3. Radio sources

Radio sources are powered by synchrotron radiation created when material is ejected in presence of strong magnetic fields. Since the discovery of the first radio source in 1944, named quasar (quasi-stellar radio source) due to its strong radio signal and stellar appearance, many types of radio sources were detected. The common point of all types is the extremely violent explosions that give rise to the radio emission. These sources are thus called Active Galactic Nucleis (AGNs) and include Seyfert galaxies, Fanaroff–Riley galaxies, Radio galaxies and Blazars.

It is now well established that the appearance of AGNs depends strongly on orientation. Classes of apparently different AGNs may be intrinsically similar, the difference being related to the viewing angles w.r.t. the l.o.s. This is the unified scheme of AGNs. The current paradigm is the following. The central engine is a supermassive black hole. An equatorial accretion disk provides means for funnelling matter onto the black hole. At this level, fast moving clouds emit Doppler-broadened lines while more distant clouds emit narrower lines. Finally, an optically thick screen (commonly idealised as a torus) obscures the central continuum and broad-line emission along some l.o.s. Some fraction of AGNs (about 10%) are radio-loud due to the additional presence of a relativistic jet, roughly perpendicular to the disk. When AGNs are seen edge-on, due to the obscuration of the central part, only the narrow-line emitting clouds are seen leading to the so-called Type 2 AGNs. When viewed face-on, broad-lines are visible (Type 1 AGNs). The unified model is based on the high anisotropy of the emission in the inner part of AGNs, implying widely different observational properties for different aspect angles. In the unified scheme, spiral galaxies Seyfert 1 and Seyfert 2 have been unified. As regards to the radio-loud objects, Fanaroff–Riley type I have been unified with BL Lacertae Objects (a sub-class of Blazars) while Fanaroff–Riley type II have been unified with radio quasars. Flat-Spectrum Radio Quasars (FSRQ, the second sub-class of blazars) are thought to be oriented at relatively small angle ($\theta < 15$ degrees) w.r.t. the l.o.s. The galaxy host of blazars, radio-loud quasars or radio galaxies is an elliptical, the difference being in the orientation of the relativistic jet w.r.t. the l.o.s. (it is coming at us, from at us to about 45 degrees, and in the plane of the sky respectively). Two other aspects characterise the radio sources: their variability (that can be violent in case for example of blazars), explained in some cases by shocks in an aligned relativistic jet, and their polarisation. The unification of radio sources is a very active field. The results are promising, however, attempts to link the (nowadays) separate unified schemes for high and low-luminosity radio-loud AGNs as well as for radio-loud and radio-quiet AGNs are still a major challenge. And moreover, effects of evolution of radio-sources are still not well understood and difficult to include in such unified pictures.

At frequencies lower than 200–300 GHz, the most relevant foreground hampering the detection of intrinsic CMB anisotropies in the radio galaxy domain is constituted by the radio-loud AGNs including flat or inverted spectrum radio galaxies and blazars. Flat spectrum radio sources include compact radio galaxies, radio-loud quasars and BL Lacertae; inverted spectrum radio sources include the so-called GHz Peaked Spectrum Radio Sources (GPS) as those characterised by advection-dominated emission. As an example, the GPS radio-sources (e.g., [42]), under-represented in the low frequency surveys, are expected to come out in mm surveys.

However, the radio-loud AGNs, since they are quite rare, will not be a threat for studies of CMB anisotropies (see Fig. 4), but we may expect that the future mm surveys will provide key informations on ‘standard’ steep- and flat-spectrum sources and will play an increasingly important role in investigating the rare, but very interesting, population of sources with non-standard spectra such as GPS, blazars and low-advection sources. Both the earliest (GPS sources) and latest (low accretion rates or low radiative efficiency sources with inverted radio spectra) stage phases of nuclear activity can be more clearly investigated in the mm range.

Finally, in the framework of extracting the power spectrum of CMB polarisation fluctuations, polarisation of extragalactic radio sources is an important issue [43]. Flat spectrum radio sources are typically 4–7% polarised at cm and mm wavelengths. However, as shown by [33] the main limitations to CMB polarisation measurements will come from the Galactic emission, not from extragalactic radio sources.

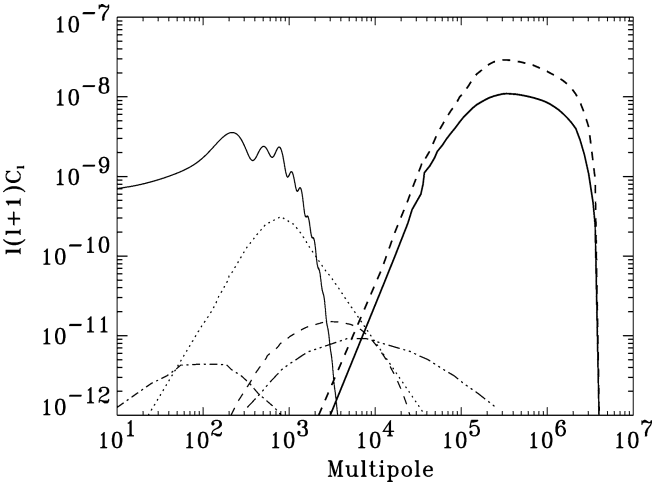

Fig. 5. Power spectrum of the temperature fluctuations taken from the literature by [45]. The solid thin line represents the CMB primary anisotropies in a standard CDM model. The thick solid and dashed lines represent the KSZ from BH-seeded proto-galaxies in $\Omega = 1$ and $\Omega = 0.3$ models respectively. The triple-dot-dashed line is the OV power spectrum. The dashed and dot-dashed lines represent respectively the galaxy cluster KSZ effect and the RS effect. The dotted line is an upper limit for the IHR effect.

4.4. SZ effect from black-hole seeded proto-galaxies

We end the discussion on the CMB extragalactic foregrounds at the scale of galaxies by a more speculative contaminant, provided by the SZ effect from proto-galaxies. Previous studies have evaluated the global Compton distortion of a population of galaxies in the virialised regime and found it much smaller than the COBE/FIRAS limit. In contrast, there can exist a regime in which the proto-galaxies are seeded by super-massive black holes (BH) that power the central nucleus (as suggested by observations of galactic nuclei, e.g., [44]). In this picture, the proto-galaxy might undergo a very active phase during which the surrounding medium is shocked and heated up to very high temperatures. The outflow, driven by the BH activity, expands and shock-heats proto-galactic gas; it then interacts with the inter-galactic medium (IGM). Three regimes may be considered: (1) the high density region of the proto-galaxy; (2) the low density IGM (cf. IHR, Section 2.2) and (3) the thin compressed layer (four times denser than the IGM) induced by the front shock. During the first phase, the proto-galactic matter is shock-heated up to a few 10^8 K and cools down to 10^5 K. It Compton scatters the CMB photons and induces spectral distortions and temperature anisotropies through the SZ effect. Contrary to the virialised phase, the regime of BH activity induces larger distortions. The global Compton parameter due to a population of BH-seeded proto-galaxies can be as large as the galaxy cluster contribution. The SZ anisotropies due to such a population might constitute the major source of CMB fluctuations on very small angular scales (sub-arcseconds to arcseconds, see Fig. 5).

5. Conclusion

To conclude, we present in Figs. 4 and 5 the predicted angular power spectrum of all major extragalactic contributions to the CMB primary anisotropies.

Fig. 4 shows the extragalactic point source contamination at 100 GHz. Poisson distribution of extragalactic point sources produces a simple white-noise power spectrum (same power in all multipoles) which translates in lines proportional to l^2 in Fig. 4. At 100 GHz, the radio sources dominate. In this case, the Poisson fluctuations are dominated by the brightest sources just below the detection limit (at shorter wavelengths the fluctuations are rather dominated by the numerous faint evolving dusty galaxies). Therefore, the level of the fluctuations highly depends on the flux limit at which sources are identified and removed. We assume here that this flux is 1 Jy. We see from Fig. 4 that the Poisson fluctuations hamper the detection of the CMB anisotropies only at large multipoles ($l \geqslant 2000$). At lower frequencies, the contamination becomes more severe. For example, at 30 GHz, the Poisson fluctuations of radio sources are a serious limitation to the CMB measurements for $l \geqslant 500$. At higher frequencies, the contribution of dusty galaxies increases (they have almost the same level as radio sources at 217 GHz) but their contamination stays important only for $l \geqslant 2000$.

In addition to the Poisson distribution, the clustering of extragalactic sources produces extra power. The clustering term is dominated by the numerous faint sources (while the Poisson one is dominated by the brightest sources just below the detection

limit). The clustering strength depends on the bias at the relevant redshift range. Studying the clustering provides valuable information on the formation of bulges and ellipticals, as well as potentially QSOs, thereby providing clues on the physical relations between dark matter and baryons when galaxies formed. We see from Fig. 4 that adding the clustering does not change significantly the level of contamination at 100 GHz. This is no more true at higher frequencies. For example, at 353 GHz, the contamination becomes very large for l greater than about 400 [46]. Indeed, [47] pointed out that, if the far-IR selected galaxies cluster in a similar manner as Lyman Break Galaxies, they may produce CIB fluctuations at 353 GHz comparable to those of the CMB at scales of 5 to 8 arcminutes (and by far larger than the *Planck* instrumental noise).

We compare the power spectra of the major sources of secondary anisotropies in Fig. 5 to the primary CMB fluctuations (thin solid line). In each case, we choose from the literature the most extreme cases as an upper limit to the contamination of the CMB. The primary anisotropies dominate at scales larger than the damping around 5 arcminutes. At intermediate scales, several effects take place among which the IHR (dotted line), the OV (triple-dot-dashed line), the RS (dot-dashed line) and the KSZ effects (dashed line). We do not plot the TSZ power spectrum of galaxy clusters, which is one order of magnitude larger than the KSZ, since it can be distinguished through its spectral signature. At very small scales (arcsecond and sub-arcsecond scales), the anisotropies are quite dominated by the proto-galactic contribution both in $\Omega = 1$ and $\Omega = 0.3$ models (thick solid and dashed lines respectively). The TSZ power spectrum of the BH-seeded protogalaxies is not plotted in this figure. It is more than one order of magnitude smaller than the KSZ due to the efficiency of the cooling which lowers the temperature down to a few 10^5 K. The very early shock-heated proto-galaxies might constitute the major source of CMB power at the arcsecond scales; they might be detected and measured by future long baseline interferometric instruments.

Acknowledgements

GL thanks Luigi Toffolatti for providing with the radio source counts and gratefully acknowledges the fruitful collaboration with Michel Piat.

References

[1] M. Birkinshaw, Phys. Rep. 310 (1999) 97.
[2] J. Carlstrom, G. Holder, A. Reese, Annu. Rev. Astron. Astrophys. 40 (2002) 643.
[3] A.D. Dolgov, S.H. Hansen, S. Pastor, D.V. Semikoz, Astrophys. J. 554 (2001) 74.
[4] J.-M. Lamarre, et al., Astrophys. J. 507 (1998) 5.
[5] R.A. Sunyaev, Ya.B. Zel'dovich, Annu. Rev. Astron. Astrophys. 18 (1980) 537.
[6] N. Aghanim, K.M. Górski, J.L. Puget, Astron. Astrophys. 374 (2001) 1.
[7] L. Grego, et al., Astrophys. J. 552 (2001) 2.
[8] E. Pointecouteau, et al., Astrophys. J. 552 (2001) 42.
[9] E.D. Reese, et al., Astrophys. J. 581 (2002) 53.
[10] D. Barbosa, J.G. Bartlett, A. Blanchard, J. Oukbir, Astron. Astrophys. 314 (1996) 13.
[11] Z. Haiman, J.J. Mohr, G.P. Holder, Astrophys. J. 552 (2001) 545.
[12] A. da Silva, et al., Mon. Not. R. Astron. Soc. 317 (2000) 37.
[13] V. Springel, M. White, L. Hernquist, Astrophys. J. 549 (2001) 681.
[14] D.J. Fixsen, et al., Astrophys. J. 473 (1996) 576.
[15] R.H. Becker, et al., Astron. J. 122 (2001) 2850.
[16] J.E. Gunn, B.A. Peterson, Astrophys. J. 142 (1965) 1633.
[17] A. Kogut, et al., Astrophys. J. (Suppl.) 148 (2003) 161.
[18] N. Aghanim, F.-X. Désert, J.-L. Puget, R. Gispert, Astron. Astrophys. 311 (1996) 1.
[19] A. Gruzinov, W. Hu, Astrophys. J. 508 (1998) 435.
[20] A.J. Benson, A. Nusser, N. Sugiyama, C.G. Lacey, Mon. Not. R. Astron. Soc. 320 (2001) 153.
[21] M. Bruscoli, A. Ferrara, E. Scannapieco, Mon. Not. R. Astron. Soc. 330 (2002) L43.
[22] J.P. Ostriker, E.T. Vishniac, Astrophys. J. 306 (1986) L51.
[23] E.T. Vishniac, Astrophys. J. 322 (1987) 597.
[24] S. Dodelson, J.M. Jubas, Astrophys. J. 439 (1995) 503.
[25] A.H. Jaffe, M. Kamionkowski, Phys. Rev. D 58 (1998) 043001.
[26] U. Seljak, Astrophys. J. 460 (1996) 549.
[27] M. Birkinshaw, S.F. Gull, Nature 302 (1983) 315.
[28] N. Aghanim, S. Prunet, O. Forni, F.R. Bouchet, Astron. Astrophys. 334 (1998) 409.
[29] J.E.G. Devriendt, B. Guiderdoni, R. Sadat, Astron. Astrophys. 350 (1999) 381.
[30] D. Elbaz, et al., Astron. Astrophys. 384 (2002) 848.
[31] G. Lagache, H. Dole, J.-L. Puget, Mon. Not. R. Astron. Soc. 338 (2003) 55.

[32] L. Toffolatti, F. Argueso Gòmez, G. De Zotti, et al., Mon. Not. R. Astron. Soc. 297 (1998) 117.
[33] L. Toffolatti, G. De Zotti, in: A. de Oliveira-Costa, M. Tegmark (Eds.), Microwave Foregrounds, ASP Conf. Ser. 181 (1999).
[34] B.T. Soifer, G. Neugebauer, Astron. J. 101 (1991) 354.
[35] J.-L. Puget, et al., Astron. Astrophys. 308 (1996) 5.
[36] B. Guiderdoni, et al., Nature Lett. 390 (1997) 257.
[37] D.J. Fixsen, et al., Astrophys. J. 508 (1998) 123.
[38] G. Lagache, et al., Astron. Astrophys. 344 (1999) 322.
[39] D. Schlegel, et al., Astrophys. J. 500 (1998) 525.
[40] M.G. Hauser, R.G. Arendt, T. Kelsall, et al., Astrophys. J. 508 (1998) 25.
[41] G. Lagache, et al., Astron. Astrophys. 355 (2000) 17.
[42] M. Tornikoski, et al., Astron. J. 1739 (2000) 2278.
[43] M. Tucci, et al., astro-ph/0307073.
[44] J. Magorrian, et al., Astron. J. 115 (1998) 2285.
[45] N. Aghanim, C. Balland, J. Silk, Astron. Astrophys. 357 (2000) 1.
[46] L. Knox, et al., Astrophys. J. 550 (2001) 7.
[47] D. Scott, M. White, Astron. Astrophys. 346 (1999) 1.
[48] M.J. Rees, D.W. Sciama, Nature 511 (1968) 611.
[49] R.K. Sachs, A.M. Wolfe, Astrophys. J. 147 (1967) 73.